AIP | The Journal of Chemical Physics

High resolution rotational analysis of the B3Π–X3Δ (1,0) band of titanium monoxide

Claude Amiot, El Mehdi Azaroual, Paul Luc, and Raymond Vetter

Citation: J. Chem. Phys. 102, 4375 (1995); doi: 10.1063/1.469486
View online: http://dx.doi.org/10.1063/1.469486
View Table of Contents: http://jcp.aip.org/resource/1/JCPSA6/v102/i11
Published by the American Institute of Physics.

High resolution rotational analysis of the $B\ ^3\Pi - X\ ^3\Delta$ (1,0) band of titanium monoxide

Claude Amiot, El Mehdi Azaroual, Paul Luc, and Raymond Vetter
Laboratoire Aimé Cotton, C.N.R.S. II, 91405 Orsay Cedex, France

(Received 3 October 1994; accepted 7 December 1994)

The $B\ ^3\Pi - X\ ^3\Delta$ (1,0) band of titanium monoxide has been studied at sub-Doppler resolution (0.002 cm^{-1}) by crossing a beam of TiO molecules with a cw tunable laser beam and by collecting the laser-induced fluorescence. The rotational structure of 42 branches belonging to the $^3\Pi - ^3\Delta$ transition has been analyzed up to rotational quantum numbers equal to 94. Spectroscopic data have been reduced to a set of 24 molecular constants, using a case (a) effective Hamiltonian. The rotational, spin–orbit and Λ-doubling constants are discussed in terms of the leading configurations which give rise to the $X\ ^3\Delta$ and $B\ ^3\Pi$ electronic states. It is shown that for the B state, existing *ab initio* calculations are not able to reproduce the second order spin–orbit effect and the Λ doubling effect.

I. INTRODUCTION

Titanium monoxide is the most abundant of the $3d$ oxides present in the spectra of cool M and S class stars.[1] It is used for spectral classification of these stars on the MK system,[2,3] the distribution of intensities in the rotational structure of TiO bands being a test to determine the temperature of stellar atmospheres.[4] This great importance in astrophysics has led to numerous spectroscopic studies.[5] TiO is also the simplest transition metal oxide known which involves d electrons in chemical bonding, justifying its interest in quantum chemistry.

Spectroscopy and bonding of the diatomic $3d$ transition metal oxides, including TiO, have been reviewed recently by Merer.[6] The observed electronic states are well represented by single configurations, $(8\sigma)^2\ (3\pi)^4\ (9\sigma)^1\ (1\delta)^1$ for the $X\ ^3\Delta$ ground state and $(8\sigma)^2\ (3\pi)^4\ (1\delta)^1\ (4\pi)^1$ for the $B\ ^3\Pi$ excited state.

Since its discovery by Cohen and Dunér in 1943,[7] the $B-X$ (or γ') band system has been studied mainly by Hocking *et al.*[8] and by Gustavsson *et al.*[9] These two studies were Doppler-limited, restricting the assignment of rotational quantum numbers to $J'' \leqslant 55$. Owing to the sub-Doppler resolution (0.002 cm^{-1} or 60 MHz) and to the high signal-to-noise ratio achieved in the present experiment, the rotational analysis of the $B\ ^3\Pi - X\ ^3\Delta$ (1,0) band has been extended up to $J''=94$. Most lines in the highly congested regions (heads in the sub-bands) are resolved for the first time, and the 3 sub-bands which are possible for a $^3\Pi - ^3\Delta$ transition are observed.

II. EXPERIMENTAL PROCEDURE

The experimental procedure has been described in detail in previous publications.[10,11] Briefly, an effusive beam of TiO molecules is produced by heating at 2200 K a tungsten crucible filled with TiO powder. The beam is perpendicularly crossed by a cw single mode tunable dye laser beam operating with Rh6G. The subsequent laser-induced fluorescence is collected by a parabolic mirror whose focus coincides with the crossing volume; it is then detected by a photomultiplier through a series of broad band optical filters, whose role is to eliminate stray light in the collision chamber and part of the blackbody radiation emitted by the oven at high temperature. This radiation is further eliminated by chopping the laser beam and using a lock-in amplifier. The laser-induced fluorescence spectrum is recorded by tuning the laser frequency over the $B\ ^3\Pi - X\ ^3\Delta$ (1,0) absorption band of TiO, by successive steps of 1 cm^{-1} between 16 800 and 17 200 cm^{-1}. The wave-number calibration is obtained through I_2 absorption lines used as calibration standards[12] and by narrow reference fringes provided by a spherical Fabry–Perot etalon (free spectral range: 0.025 cm^{-1}). The final resolution of the experiment (0.002 cm^{-1}) is mainly due to the residual Doppler broadening associated with the angular aperture of the two beams (1°), to the finite lifetime of the excited level and to the jitter of the laser. At least four recordings of the same spectral region were performed to detect mode hops of the laser and to determine the internal coherence of the wave numbers (0.001 cm^{-1}).

III. DESCRIPTION OF THE SPECTRA

Because of spin–orbit coupling, the $B\ ^3\Pi$ and $X\ ^3\Delta$ states of $^{48}Ti\ ^{16}O$ are split into three sub-states. Since the triplet splitting is much larger in the $X\ ^3\Delta$ state (101 cm^{-1}) than in the $B\ ^3\Pi$ one (21 cm^{-1}), a band consists in three distinct, case (a) allowed sub-bands labelled as $^3\Pi_0 - ^3\Delta_1$, $^3\Pi_1 - ^3\Delta_2$, and $^3\Pi_2 - ^3\Delta_3$. The $\cdots\ (1\delta)^1\ (4\pi)^1\ B\ ^3\Pi$ state has such a small spin–orbit coupling because it is the difference between the one for 1δ and for 4π electrons. As a consequence, the $B\ ^3\Pi$ state uncouples rapidly with increasing rotation to case (b), so that satellite branches ($\Delta\Sigma=0$) become allowed.

Figure 1 shows a portion of the spectrum between 17 052.5 cm^{-1} and 17 053 cm^{-1}. It shows the band head of the $R_{32\,f}$ satellite branch which occurs near $J=29$.

The branches are split into two components, noted as usually by (e) and (f),[8] as a result of Λ doubling in the $B\ ^3\Pi$ state. The Λ-doubling in the $^3\Delta$ state was found negligible, even at the high resolution of the recorded spectra.

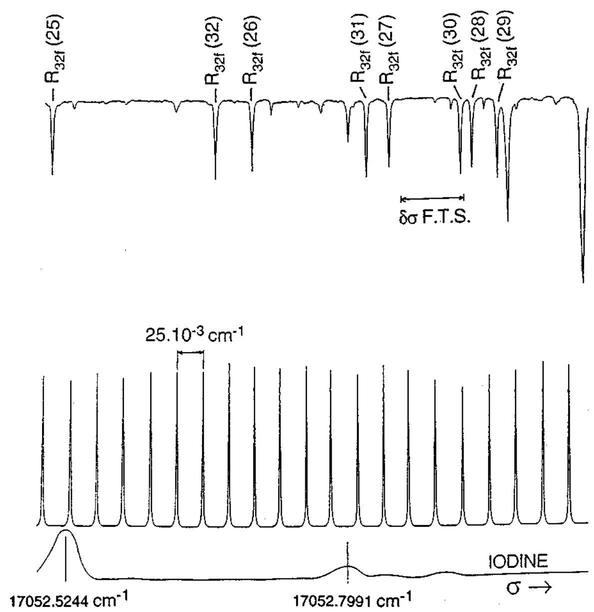

FIG. 1. Absorption spectrum of TiO between 17 052.5 cm^{-1} and 17 053 cm^{-1} (upper trace), with reference fringes 25×10^{-3} cm^{-1} apart (medium trace) and I_2 absorption spectrum (lower trace). This section of the spectrum shows the band head of the $R_{32}f$ branch, which occurs for $J=29$. The quantity noted $\delta\sigma$ FTS represents the linewidth observed in the FTS measurements of Ref. 9. The label 1,2,3 is used in the $B\ ^3\Pi$ state to note the $^3\Pi_{\Omega=0}$, $^3\Pi_{\Omega=1}$, $^3\Pi_{\Omega=2}$ sublevels and in $X\ ^3\Delta$ to indicate the $^3\Delta_{\Omega=1}$, $^3\Delta_{\Omega=2}$, $^3\Delta_{\Omega=3}$ sublevels. $R_{32}f(29)$ is written for the satellite line $^3\Pi_{\Omega=2}(J'=30,f)\leftarrow{}^3\Delta_{\Omega=2}(J''=29,f)$.

Figure 2 shows directly the Λ-doubling in the $B\ ^3\Pi_2$ sublevel observed through the Q_3 branches for $J=26$ and through the P_3 branches for $J=10$. In both figures, the quantity $\delta\sigma$ FTS represents the linewidth of the spectrum recorded by Fourier transform spectroscopy[9] with Doppler-limited sources. These two spectra clearly show that the combination of sub-Doppler resolution and high signal to noise leads to detailed information about congested spectra.

IV. ENERGY MATRICES FITTING PROCEDURE

An effective Hamiltonian has been written using the $\mathbf{R}^2$ formalism[13,14] where $\mathbf{R}=\mathbf{J}-\mathbf{L}-\mathbf{S}$ as

$$H_{\mathrm{eff}}=H_{\mathrm{rot}}+H_{\mathrm{cd}}+H_{\mathrm{so}}+H_{\mathrm{cdso}}+H_{\mathrm{sr}}+H_{\mathrm{LD}}+H_{\mathrm{cd}\Lambda\mathrm{D}}.$$

The five first terms are the rotational, centrifugal distortion, spin–orbit, centrifugal distortion of spin–orbit and spin–rotation components of the total Hamiltonian H_{eff}. The last two terms are the Λ-doubling and its centrifugal distortion component. They have the following form:[15]

$$H_{\mathrm{rot}}=B\mathbf{R}^2$$

$$H_{\mathrm{cd}}=-D\mathbf{R}^4+H\mathbf{R}^6$$

$$H_{\mathrm{so}}=AL_zS_z+2/3\lambda(3S_z^2-\mathbf{S}^2)$$

$$H_{\mathrm{cdso}}=1/2A_D[L_zS_z,\mathbf{R}^2]_++1/3\lambda_D[3S_z^2-\mathbf{S}^2,\mathbf{R}^2]_+ +1/2A_H[L_zS_z,\mathbf{R}^4]_++1/3\ \lambda_H[S_z^2-\mathbf{S}^2,\mathbf{R}^4]_+$$

$$H_{\mathrm{sr}}=\gamma\mathbf{R}.\mathbf{S}$$

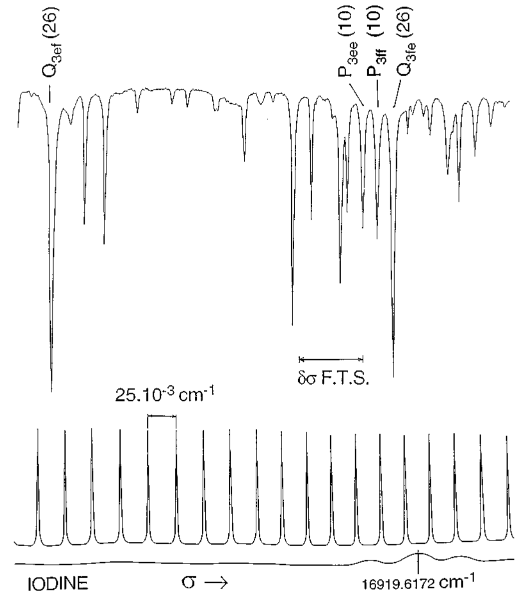

FIG. 2. Absorption spectrum of TiO around 16 919.5 cm^{-1} (upper trace) with reference fringes and I_2 absorption spectrum as in Fig. 1. This section of the spectrum shows the Λ-doubling observed in the Q_3 branch for $J=26$ and the Λ-doubling observed in the P_3 branch for $J=10$. For main branches, only one subscript is used. For example $P_{3ff}(10)$ means $^3\Pi_{\Omega=2}(J'=9,f)\leftarrow{}^3\Delta_{\Omega=3}(J''=10,f)$.

$$H_{\Lambda\mathrm{D}}=1/2(o+p+q)(S_+^2+S_-^2)-1/2(p+2q)\times(J_+S_++J_-S_-)+1/2q(J_+^2+J_-^2)$$

$$H_{\mathrm{cd}\Lambda\mathrm{D}}=1/4D_{o+p+q}[S_+^2+S_-^2,\mathbf{R}^2]_+-1/4D_{p+2q}[J_+S_+ +J_-S_-,\mathbf{R}^2]_++1/4D_q[J_+^2+J_-^2,\mathbf{R}^2]_+ +1/4H_{o+p+q}[S_+^2+S_-^2,\mathbf{R}^4]_+-1/4H_{p+2q}[J_+S_+ +J_-S_-,\mathbf{R}^4]_++1/4H_q[J_+^2+J_-^2,\mathbf{R}^4]_+.$$

The symbol $[x,y]_+$ is the anticommutator $xy+yx$ which is necessary to preserve the Hermitian form of the matrices. The parameters in this effective Hamiltonian are

(1) the rotational constant B with its first and second centrifugal distortion corrections D and H;
(2) the first-order spin–orbit constant A, the second-order constant λ and the associated first and second centrifugal distortion corrections A_D,A_H and λ_D,λ_H;
(3) the spin–rotation constant γ;
(4) the lambda-doubling constants, introduced only for the $^3\Pi$ electronic state, $(o+p+q)$, $(p+2q)$ and q with its first and second order centrifugal distortion corrections D_{o+p+q},H_{o+p+q}, D_{p+2q},H_{p+2q} and D_q,H_q.

Taking the usually negligible Λ-doubling in the $X\ ^3\Delta$ state into account and using a case (a) basis set ($|\Lambda;\ S\Sigma;\ J\Omega\rangle$), one obtains the matrix representation of the Hamiltonian for parity-independent elements:

$$\langle\Lambda,\Sigma=1,J|H|\Lambda,\Sigma=1,J\rangle=T+A\Lambda+2/3\ \lambda-\gamma+(B+A_D\Lambda+2/3\ \lambda_D)(x-\Lambda^2-2\Lambda)-D[x^2+2x-2\Lambda x(\Lambda+2)+2\Lambda(\Lambda-1)+\Lambda^3(\Lambda+4)];$$

$$\langle \Lambda,\Sigma=0,J|H|\Lambda,\Sigma=0,J\rangle$$
$$=T-4/3\ \lambda-2\gamma+(B-4/3\ \lambda_D)(x-\Lambda^2+2)$$
$$-D[x^2+8x-2\Lambda^2(x+4)+\Lambda^4+4)];$$

$$\langle \Lambda,\Sigma=-1,J|H|\Lambda,\Sigma=-1,J\rangle$$
$$=T-A\Lambda+2/3\ \lambda-\gamma+(B-A_D\Lambda+2/3\ \lambda_D)$$
$$\times(x-\Lambda^2+2\Lambda)-D[x(x+2)-2\Lambda x(\Lambda-2)$$
$$+2\Lambda(\Lambda+1)+\Lambda^3(\Lambda-4)];$$

$$\langle \Lambda,\Sigma=0,J|H|\Lambda,\Sigma=1,J\rangle$$
$$=T-\sqrt{2[x-\Lambda(\Lambda+1)]}[B-1/2\gamma+1/2A_D\Lambda-1/3\lambda_D$$
$$-2D(x-\Lambda-\Lambda^2+1)];$$

$$\langle \Lambda,\Sigma=-1,J|H|\Lambda,\Sigma=1,J\rangle$$
$$=T-2D\sqrt{(x-\Lambda^2+\Lambda)(x-\Lambda^2-\Lambda)};$$

$$\langle \Lambda,\Sigma=1,J|H|\Lambda,\Sigma=0,J\rangle$$
$$=T-\sqrt{2[x-\Lambda(\Lambda-1)]}[B-1/2\ \gamma-1/2\ A_D\Lambda$$
$$-1/3\ \lambda_D-2D(x+\Lambda-\Lambda^2+1)];$$

where $x=J(J+1)$.

The following higher order elements have been used for the $^3\Pi$ state, together with the parity-dependent matrix elements: (These matrix elements are comparable with the ones indicated in Ref. 15, but the elements relative to the hyperfine structure have been removed. We are indebted to Professor Merer for indicating a misprint in Table II of Ref. 15.)

$$\langle \Lambda,\Sigma=1,J|H|\Lambda,\Sigma=1,J\rangle$$
$$=H(x^3-3x^2+5x-7)+A_H(x^2-5x+7)$$
$$+2/3\ \lambda_H(x^2-7x+11)+H_qx(x-2);$$

$$\langle \Lambda,\Sigma=0,J|H|\Lambda,\Sigma=0,J\rangle$$
$$=H(x^3+15x^2-5x+5)-2A_H$$
$$-2/3\ \lambda_H(2x^2+5x+1)\pm x[1/2q+D_{p+2q}$$
$$+1/2\ D_q(x+1)]+1/2H_qx(x^2+6x-5)$$
$$+H_{p+2q}2x(x+1)+2xH_{o+p+q};$$

$$\langle \Lambda,\Sigma=-1,J|H|\Lambda,\Sigma=-1,J\rangle$$
$$=H(x^3+9x^2+9x+1)-A_H(x^2+3x+1)$$
$$+2/3\lambda_H(x^2+x+1)\pm[(o+p+q)+D_{o+p+q}(x+1)$$
$$+D_{p+2q}x]+H_qx(x-1)+H_{p+2q}2x(x+1)$$
$$+H_{o+p+q}(x^2+4x+1);$$

$$\langle \Lambda,\Sigma=0,J|H|\Lambda,\Sigma=1,J\rangle$$
$$=-\sqrt{2(x-2)}[H(3x^2-2x+3)+A_H(x-2)$$
$$-2/3\lambda_H(x+2)\pm x/2\ D_q+1/2\ H_qx(2x-1)$$
$$+1/2\ xH_{p+2q}];$$

TABLE I. TiO molecular parameters (in cm^{-1}). Number of data points: 1207, root mean square of the fit: 0.0021 cm^{-1}. The numbers in parentheses are the uncertainties (one standard deviation) in units of the last quoted decimal digit. **T* value constrained to zero in the matrix elements of the $X\ ^3\Delta$ ($v=0$) level.

	$X\ ^3\Delta$ ($v=0$)		$B\ ^3\Pi$ ($v=1$)	
T	[0]*		17 010.830 92	(15)
A	50.650 947	(89)	20.813 35	(23)
λ	1.747 21	(10)	−0.930 34	(23)
$10^2\ \gamma$			2.4896	(52)
B	0.533 808 1	(25)	0.502 855 8	(52)
$10^7\ D$	6.0274	(52)	6.8954	(55)
$10^4\ A_D$	−0.264 73	(79)	−1.148	(26)
$10^6\ \lambda_D$	0.49	(10)	−3.74	(64)
$10^{13}\ H$			0.77	(10)
$10^9\ A_H$			−6.47	(14)
$10^9\ \lambda_H$			−0.61	(15)
$o+p+q$			−0.591 92	(25)
$10^2\ (p+2q)$			2.671 70	(94)
$10^3\ q$			0.296 54	(34)
$10^6\ D_{o+p+q}$			1.40	(41)
$10^7\ D_{p+2q}$			1.082	(32)
$10^{10}\ D_q$			−7.86	(87)
$10^{10}\ H_{o+p+q}$			5.6	(10)

$$\langle \Lambda,\Sigma=-1,J|H|\Lambda,\Sigma=1,J\rangle$$
$$=\sqrt{x(x-2)}[H(6x-2)-2/3\lambda_H$$
$$\pm[1/2\ q+1/2\ D_q(x-1)]+1/2\ H_qx^2$$
$$+H_{p+2q}(x+1)+H_{o+p+q})];$$

$$\langle \Lambda,\Sigma=-1,J|H|\Lambda,\Sigma=0,J\rangle$$
$$=-\sqrt{2x}[H(3x^2+10x-1)-A_H(x+1)-2/3\lambda_H(x+1)$$
$$\pm[(1/2\ (p+2q)+1/2\ D_q(x-1)$$
$$+1/2\ D_{p+2q}(x+1)+D_{o+p+q}]+1/2\ H_q(2x^2-1)$$
$$+1/2\ H_{p+2q}(x^2+4x+1)+3/2\ H_{o+p+q}(x+1)].$$

The other matrix elements are derived to keep the matrix symmetrical.

To interpret the experimental spectrum, the line frequencies were fitted to the differences between the eigenvalues of the Hamiltonian matrices constructed as shown above. An iterative nonlinear least-square procedure was employed with 1207 wave numbers, yielding a standard deviation of 0.0021 cm^{-1} to compare with the two older works[8,9] where standard deviations of 5×10^{-3} cm^{-1} and 10×10^{-3} cm^{-1} were, respectively, obtained. Both γ and A_D parameters were found necessary to correctly reproduce the wave numbers. The derived constants are indicated in Table I. Generally speaking, more than one order of magnitude has been gained in the determination of the lower order constants. The rotational term energy values are collected in the Appendix.

If the relative ordering e/f were changed, only the Λ-doubling parameters $o+p+q$, $p+2q$ and q and their centrifugal distortions would have a different sign, the other parameters would not be modified.

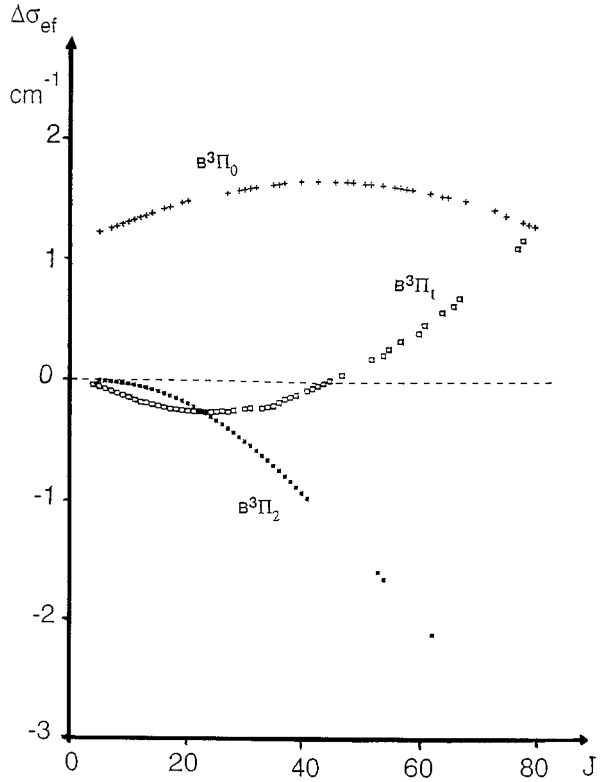

FIG. 3. Variation of the $\Delta\sigma_{ef}$ quantity as a function of J in the $B\ ^3\Pi$ ($v=1$) level (experimental data).

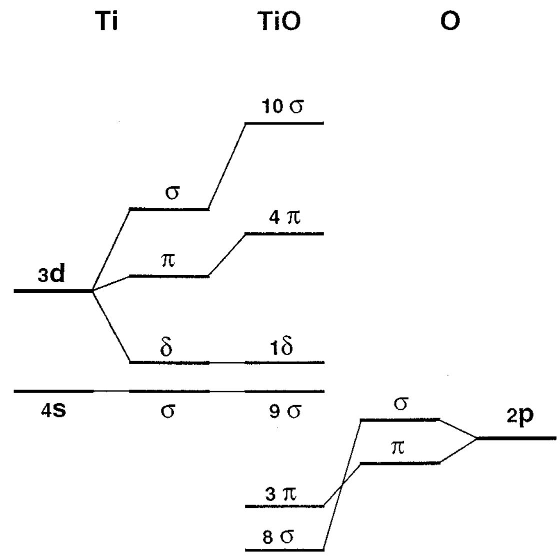

FIG. 4. The molecular orbital diagram of TiO (adapted from Ref. 6).

V. Λ-TYPE DOUBLING

As is well known,[8] the absolute sign of the Λ-splitting would require a knowledge of the parity of the individual Λ-doublet components. This can be obtained experimentally, only through the observation of a transition involving a $^3\Sigma$ state. As this is not the case in the present experiment, the notation (a) and (b) used by Merer *et al.*[8] has been kept, by setting (a) for the e parity and (b) for the f one. On the other hand, the relative signs of the Λ-doublet splittings can be determined. At high J, the coupling in the $^3\Pi$ state transforms into case (b), then, the Λ-doubling in the $B\ ^3\Pi_0$ and $^3\Pi_2$ substates becomes of the same magnitude, but its sign is opposite to that of the $^3\Pi_1$ substate. Also, for small J, the sum of the Λ-doubling in $^3\Pi_1$ and $^3\Pi_0$ is constant. Using the above informations, it has been possible to plot the energy difference $\Delta\sigma_{ef}$ between the e and f components for each of the three $B\ ^3\Pi$ substates, as a function of J (Fig. 3). In $^3\Pi_0$, this quantity is large at low J, grows toward a maximum near $J=42$ and then decreases. In $^3\Pi_2$, the Λ-doubling increases more rapidly with J than in $^3\Pi_0$ and it never reverses. These variations are basically identical to those observed for lower J in the $v=0$ level of the B state.[8]

In a recent paper, Balfour *et al.*[15] have compared the electronic structure of TiO with that of the isoelectronic molecule VN. A guessed energy level diagram showed that the lowest states of the $(\delta)^2$ configuration have a $^3\Sigma^-$ character at about 5000 cm^{-1} and a $^1\Sigma^+$ character at about 14 000 cm^{-1}, both below the $B\ ^3\Pi$ state. As the Λ-doubling in the $B\ ^3\Pi_0$ component seems to be due mainly to spin–orbit interactions with the $^3\Sigma^-_{0e}$ and $^1\Sigma^+_e$ states (cf. Chap. VI), the $B\ ^3\Pi_{0e}$ component is shifted towards higher frequencies, leading to a positive $\Delta\sigma_{ef}$ value, as represented in Fig. 3. Obviously, the spin–orbit interaction can occur with other electronic states arising from electron configurations such as π^2.

VI. DISCUSSION

The molecular orbital diagram of TiO, as reported by Merer, is shown in Fig. 4. The 8σ and 3π molecular orbitals (m.o.) are oxygen-based orbitals, slightly bonding combinations of O $2p\sigma$ and O $2p\pi$ atomic orbitals (a.o.) with Ti $3d\sigma$ and Ti $3\,d\pi$ a.o. respectively. The proportion of Ti $3d$ character is calculated to be about 15%.[17] The 9σ m.o. is essentially the Ti 4σ a.o., while the 4π m.o. is an antibonding combination of the Ti $3d\pi$ and O $2p\pi$ a.o., being largely Ti $3d$ in character. The (1δ) m.o. is predicted to be essentially a pure Ti centered $3\,d\delta$ a.o.

There have been two *ab initio* calculations on the low-lying electronic states of TiO[16,17] indicating that the electron configuration giving rise to this $X\ ^3\Delta$ state is $\cdots(8\sigma)^2\,(3\pi)^4\,(9\sigma)^1\,(1\delta)^1$. Based upon the intensity of the $B-X$ system, it is most likely that the excited $B\ ^3\Pi$ electronic state configuration differs from that of the ground state, by the promotion of the 9σ electron into a 4π m.o., which is primarily a Ti centered $3\,d\pi$ a.o. . The primary configuration of the B state is then predicted to be mainly $\cdots(8\sigma)^2\,(3\pi)^4\,(1\delta)^1\,(4\pi)^1$, although no population analysis of the orbitals was reported for this configuration.[17]

In the following, the validity of the above mentioned electron configurations will be put into evidence by calculating the first-order spin–orbit constants, but it will be shown that the second-order spin–orbit and Λ-doubling parameters do not lead to a good agreement and that configuration mixing must be taken into account.

A. The first-order spin–orbit constants

Using the microscopic spin–orbit Hamiltonian $H_{\rm so} = \Sigma a_i \mathbf{l_i} . \mathbf{s_i}$ and a single configuration representation for the electronic states, it is possible to relate the observed spin–orbit parameters to the one-electron ones a_i.

In the absence of higher order effects, the spin–orbit intervals between the degenerate multiplet components are equal to $A\Lambda$. In the present study $A\Lambda = 101.30\ \mathrm{cm}^{-1}$ for the $X\ ^3\Delta$ ($\Lambda=2$) state and $A\Lambda = 20.81\ \mathrm{cm}^{-1}$ for the $B\ ^3\Pi$ ($\Lambda=1$) state (Table I). The wave functions for the $X\ ^3\Delta\ \sigma^1\ \delta^1$ and $B\ ^3\Pi\ \delta^1 \pi^1$ electron configurations are $|^3\Delta_{\Omega=3}\rangle = |\sigma\alpha\delta^+\alpha\rangle$ and $|^3\Pi_{\Omega=2}\rangle = |\delta^+\alpha\pi^-\alpha|$.[18] The diagonal matrix elements are then calculated as

$$\langle ^3\Delta_3 | H_{\rm so} | ^3\Delta_3\rangle = \hat{a}_\delta,$$

$$\langle ^3\Pi_2 | H_{\rm so} | ^3\Pi_2\rangle = \hat{a}_\delta - (1/2)\hat{a}_\pi.$$

The $X\ ^3\Delta$ state is well isolated, so that $\hat{a}_\delta = A\Lambda = 101.302\ \mathrm{cm}^{-1}$ to compare with the value $96\ \mathrm{cm}^{-1}$ for the Ti^+ ($3d^3 4s^1$) ion.[6]

In the $B\ ^3\Pi$ state, the separation for the $\Omega=0$ and $\Omega=2$ components is equal to $2A - 1/2(o+p+q) = \hat{a}_\delta - (1/2)\hat{a}_\pi$. The numerical value of this quantity, based on the constants reported in Table I, is $21.109\ \mathrm{cm}^{-1}$ or $20.517\ \mathrm{cm}^{-1}$, whether the quantity $o+p+q$ is positive or negative. The parameter $\hat{a}_\pi$ is then equal either to 160.386 or to $161.570\ \mathrm{cm}^{-1}$, to be compared with $156.70\ \mathrm{cm}^{-1}$ for TiN.[13]

Thus, it is verified that the parameter $\hat{a}_\delta$ is equivalent to the atomic $\zeta 3d$ value, confirming that the electron configuration of the $X\ ^3\Delta$ state is $\cdots(9\sigma)^1\ (3d\delta)^1$. Similarly, the values for $\hat{a}_\pi$ in TiO and TiN indicate that the type of bonding occurring in the two molecules is almost the same, well described by the above mentioned configuration for the X state.

B. The second-order spin–orbit constants

Equal splittings between the components of a multiplet state can occur only in the absence of higher-order spin–orbit effects or spin–spin interactions.

The principal higher-order spin–orbit effect in TiO results from the singlet–triplet interaction between states coming from the same electron configuration, the $a\ ^1\Delta$ and $X\ ^3\Delta$ states for the $\sigma\delta$ configuration, or the $(\delta\pi)\ ^1\Pi$ and $B\ ^3\Pi$ states for the $\delta\pi$ configuration.

In the first case ($\sigma\delta$ configuration), the central spin component of the triplet Δ state, with $\Omega=1$, is shifted below its expected position by an amount 2λ. The spin–orbit matrix element between the $a\ ^1\Delta$ and $X\ ^3\Delta$ states is calculated as $-\hat{a}_\delta$,[15] i.e., $-101.3\ \mathrm{cm}^{-1}$. By use of the method of Balfour *et al.*,[15] the singlet–triplet separation ΔE is represented by the expression:

$$\Delta E = 2\lambda + \hat{a}_\delta^{\,2}/2\lambda.$$

With $\lambda = 1.747\ \mathrm{cm}^{-1}$ (Table I) and $|\hat{a}_\delta| = 101.3\ \mathrm{cm}^{-1}$, one finds $\Delta E = 2940.5\ \mathrm{cm}^{-1}$. The experimental value is about $3440\ \mathrm{cm}^{-1}$, indicating that some perturbation, in addition to the $^1\Delta - ^3\Delta$ one, affects the ground state. In fact, the parameter $\hat{a}_\delta$ should be increased by only 8% to correctly reproduce the observations.

A similar treatment carried out for the $(\delta\pi)\ ^1\Pi - B\ ^3\Pi$ interaction gives a matrix element $H_{12} = \langle ^1\Pi | H_{\rm SO} | B\ ^3\Pi\rangle = -[(\hat{a}_\delta + 1/2(\hat{a}_\pi)]$ of about $-181.7\ \mathrm{cm}^{-1}$ (this value is, as expected, very close to the spin–orbit constant $-173\ \mathrm{cm}^{-1}$ of the $A\ ^3\Phi$ state arising from the same $\delta\pi$ configuration). The value for the mean energy of the $^3\Pi_2$ and $^3\Pi_{0f}$ components is

$$1/2[A + (2/3)\lambda - (A - (2/3)\lambda + o + p + q)]$$

$$= 1/2[(4/3)\lambda + o + p + q].$$

The difference of this mean energy with the energy of the $^3\Pi_1$ component [equal to $(4/3)\lambda$] is

$$s = 2\lambda + 1/2(o+p+q).$$

The quantity $1/2(o+p+q)$, which is equal to $0.296\ \mathrm{cm}^{-1}$ in absolute value, is smaller than $2\lambda = -1.86\ \mathrm{cm}^{-1}$. So, whatever the sign of $o+p+q$, the quantity s is necessarily negative indicating that another interaction takes place between the $B\ ^3\Pi$ state and a new $^1\Pi$ state located below the $B\ ^3\Pi$ state. The position of the two interacting electronic states is represented by the expression[13]

$$\Delta E = s + H_{12}^{\,2}/s.$$

The derived ΔE value, about $-14\,000\ \mathrm{cm}^{-1}$, is clearly meaningless since no $^1\Pi$ state of the same configuration is found below the $B\ ^3\Pi$ one. This fact indicates that perturbations are affecting the spin structure of the state. In particular the $b\ ^1\Pi$ state (of the $9\sigma 4\pi$ configuration) at $14\,721\ \mathrm{cm}^{-1}$ has some $\delta\pi$ character.[5,6] This will increase the energy of the central $^3\Pi_1$ component of $B\ ^3\Pi$ and since the two states are close in energy, even a faint $(\delta\pi)$ mixture will shift this state more than a pure $(\delta\pi)\ ^1\Pi$ interaction.[18] The small absolute value of λ is the result of two opposing tendencies, leading to difficult predictive values.

C. The Λ doubling

Generally speaking, in $^3\Pi$ components the Λ-doubling results from rotational ($B(R)J \cdot L$ from $B(R)R^2$) $\Pi \approx \Sigma$ interactions as well as through the spin–orbit operator and also through the $S_x^2 - S_y^2$ part of the spin–spin operator.[19]

Following the method outlined by Balfour *et al.*,[15] the Λ-doubling in the $B\ ^3\Pi$ state must be due to the $^1\Sigma^+$ and $^3\Sigma^-$ states arising from electron configurations such as π^2 and δ^2.[19] For TiO, the states which are likely to contribute to the Λ-doubling are the $^3\Sigma^-$ and $^1\Sigma^+$ states arising from the configuration $(1\delta)^2$.

The interaction matrix elements are obtained as follows with the electronic wave functions for the δ^2 states:

$$|\delta^2, ^1\Sigma^+\rangle = 1/2(|\delta^-\alpha\delta^+\beta| - |\delta^-\beta\delta^+\alpha|);$$

$$|\delta^2, ^3\Sigma_0^-\rangle = 1/2(|\delta^-\alpha\delta^+\beta| + |\delta^-\beta\delta^+\alpha|);$$

$$|\delta\pi, B^3\Pi_{0e}\rangle = 1/2(|\delta^+\beta\pi^-\beta| - |\delta^-\alpha\pi^+\alpha|).$$

The following matrix elements for the spin–orbit operator are:

$$\langle \delta^2\ ^1\Sigma^+ | H_{\rm so} | B\ ^3\Pi_{0e}\rangle = -1/2\langle\delta|\hat{a}|\delta\rangle 1(1+1) - 2 = \hat{a}_\delta;$$

$$\langle \delta^2\ ^3\Sigma_0^- | H_{\rm so} | B\ ^3\Pi_{0e}\rangle = 1/2\langle\delta|\hat{a}|\delta\rangle 1(1+1) - 2 = \hat{a}_\delta;$$

TABLE II. See Appendix A.

J	F3E	F2E	F1E	F3F	F2F	F1F
1		17013.5711	16991.4321		17013.5741	16990.2458
2	17032.6204	17015.5510	16993.3617	17032.6205	17015.5599	16992.1707
3	17035.8048	17018.5222	16996.2565	17035.8050	17018.5396	16995.0585
4	17040.0475	17022.4857	17000.1170	17040.0483	17022.5141	16998.9099
5	17045.3462	17027.4433	17004.9437	17045.3481	17027.4847	17003.7256
6	17051.6981	17033.3967	17010.7376	17051.7018	17033.4526	17009.5067
7	17059.1004	17040.3476	17017.4994	17059.1067	17040.4194	17016.2542
8	17067.5498	17048.2979	17025.2301	17067.5598	17048.3863	17023.9694
9	17077.0432	17057.2491	17033.9309	17077.0582	17057.3546	17032.6535
10	17087.5776	17067.2028	17043.6028	17087.5988	17067.3255	17042.3080
11	17099.1498	17078.1603	17054.2471	17099.1[illegible]88	17078.2998	17052.9343
12	17111.7572	17090.1227	17065.8650	17111.7954	17090.2785	17064.5339
13	17125.3968	17103.0908	17078.4579	17125.4458	17103.2622	17077.1082
14	17140.0662	17117.0652	17092.0269	17140.1276	17117.2512	17090.6586
15	17155.7629	17132.0465	17106.5734	17155.8383	17132.2460	17105.1866
16	17172.4847	17148.0349	17122.0985	17172.5758	17148.2466	17120.6935
17	17190.2296	17165.0305	17138.6034	17190.3378	17165.2531	17137.1805
18	17208.9955	17183.0333	17156.0893	17209.1224	17183.2654	17154.6490
19	17228.7806	17202.0432	17174.5573	17228.9279	17202.2834	17173.1000
20	17249.5833	17222.0600	17194.0082	17249.7524	17222.3067	17192.5346
21	17271.4020	17243.0832	17214.4430	17271.5943	17243.3350	17212.9537
22	17294.2352	17265.1125	17235.8626	17294.4521	17265.3679	17234.3582
23	17318.0814	17288.1475	17258.2678	17318.3244	17288.4051	17256.7489
24	17342.9393	17312.1877	17281.6591	17343.2098	17312.4460	17280.1265
25	17368.8078	17337.2325	17306.0372	17369.1069	17337.4902	17304.4915
26	17395.6855	17363.2813	17331.4027	17396.0146	17363.5370	17329.8447
27	17423.5714	17390.3337	17357.7559	17423.9317	17390.5860	17356.1863
28	17452.4644	17418.3889	17385.0973	17452.8570	17418.6366	17383.5167
29	17482.3632	17447.4463	17413.4272	17482.7895	17447.6882	17411.8363
30	17513.2671	17477.5054	17442.7457	17513.7280	17477.7401	17441.1453
31	17545.1748	17508.5653	17473.0531	17545.6716	17508.7918	17471.4438
32	17578.0856	17540.6256	17504.3495	17578.6192	17540.8426	17502.7320
33	17611.9983	17573.6854	17536.6349	17612.5698	17573.8919	17535.0099
34	17646.9121	17607.7442	17569.9093	17647.5225	17607.9390	17568.2774
35	17682.8261	17642.8011	17604.1726	17683.4764	17642.9833	17602.5345
36	17719.7392	17678.8556	17639.4247	17720.4304	17679.0240	17637.7812
37	17757.6507	17715.9068	17675.6656	17758.3837	17716.0606	17674.0171
38	17796.5596	17753.9541	17712.8949	17797.3354	17754.0922	17711.2421
39	17836.4650	17792.9967	17751.1124	17837.2845	17793.1182	17749.4560
40	17877.3660	17833.0338	17790.3178	17878.2301	17833.1379	17788.6584
41	17919.2617	17874.0648	17830.5108	17920.1713	17874.1505	17828.8490
42	17962.1513	17916.0889	17871.6910	17963.1072	17916.1553	17870.0274
43	18006.0338	17959.1052	17913.8581	18007.0368	17959.1515	17912.1933
44	18050.9083	18003.1130	17957.0115	18051.9594	18003.1384	17955.3460
45	18096.7739	18048.1115	18001.1507	18097.8739	18048.1151	17999.4853
46	18143.6298	18094.0999	18046.2754	18144.7794	18094.0809	18044.6105
47	18191.4749	18141.0773	18092.3848	18192.6750	18141.0350	18090.7212
48	18240.3084	18189.0429	18139.4786	18241.5598	18188.9765	18137.8167
49	18290.1293	18237.9960	18187.5560	18291.4329	18237.9047	18185.8964
50	18340.9368	18287.9355	18236.6164	18342.2931	18287.8186	18234.9598
51	18392.7297	18338.8606	18286.6592	18394.1397	18338.7174	18285.0060
52	18445.5073	18390.7706	18337.6837	18446.9717	18390.6002	18336.0346
53	18499.2684	18443.6643	18389.6892	18500.7880	18443.4662	18388.0447
54	18554.0122	18497.5410	18442.6750	18555.5877	18497.3144	18441.0357
55	18609.7377	18552.3997	18496.6403	18611.3698	18552.1439	18495.0067
56	18666.4437	18608.2394	18551.5843	18668.1332	18607.9538	18549.9570
57	18724.1294	18665.0593	18607.5063	18725.8770	18664.7431	18605.8858
58	18782.7936	18722.8583	18664.4053	18784.6001	18722.5108	18662.7923
59	18842.4354	18781.6354	18722.2806	18844.3015	18781.2561	18720.6755
60	18903.0537	18841.3897	18781.1313	18904.9801	18840.9778	18779.5347
61	18964.6475	18902.1201	18840.9565	18966.6348	18901.6751	18839.3689
62	19027.2155	18963.8256	18901.7552	19029.2646	18963.3468	18900.1773
63	19090.7569	19026.5052	18963.5266	19092.8684	19025.9919	18961.9588
64	19155.2703	19090.1578	19026.2698	19157.4450	19089.6093	19024.7126
65	19220.7548	19154.7822	19089.9836	19222.9933	19154.1981	19088.4377
66	19287.2092	19220.3775	19154.6671	19289.5123	19219.7570	19153.1330
67	19354.6324	19286.9425	19220.3194	19357.0006	19286.2851	19218.7976
68	19423.0231	19354.4762	19286.9394	19425.4573	19353.7811	19285.4304
69	19492.3802	19422.9772	19354.5259	19494.8810	19422.2440	19353.0303
70	19562.7025	19492.4446	19423.0781	19565.2706	19491.6726	19421.5964
71	19633.9889	19562.8771	19492.5947	19636.6250	19562.0657	19491.1274
72	19706.2380	19634.2735	19563.0747	19708.9428	19633.4222	19561.6224
73	19779.4487	19706.6327	19634.5169	19782.2228	19705.7408	19633.0801
74	19853.6197	19779.9535	19706.9201	19856.4638	19779.0204	19705.4994
75	19928.7497	19854.2345	19780.2833	19931.6645	19853.2597	19778.8792
76	20004.8374	19929.4746	19854.6053	20007.8236	19928.4575	19853.2182
77	20081.8817	20005.6724	19929.8848	20084.9399	20004.6125	19928.5153
78	20159.8810	20082.8268	20006.1205	20163.0120	20081.7234	20004.7692
79	20238.8342	20160.9364	20083.3114	20242.0386	20159.7889	20081.9788
80	20318.7399	20239.9999	20161.4561	20322.0183	20238.8078	20160.1426
81	20399.5967	20320.0159	20240.5533	20402.9498	20318.7787	20239.2596
82	20481.4032	20400.9832	20320.6018	20484.8317	20399.7003	20319.3283
83	20564.1581	20482.9004	20401.6003	20567.6626	20481.5711	20400.3475
84	20647.8599	20565.7660	20483.5473	20651.4412	20564.3900	20482.3159
85	20732.5073	20649.5788	20566.4417	20736.1660	20648.1553	20565.2320
86	20818.0988	20734.3372	20650.2820	20821.8355	20732.8658	20649.0946
87	20904.6329	20820.0399	20735.0668	20908.4484	20818.5200	20733.9022
88	20992.1083	20906.6855	20820.7947	20996.0031	20905.1165	20819.6535
89	21080.5233	20994.2724	20907.4644	21084.4981	20992.6539	20906.3471
90	21169.8766	21082.7992	20995.0744	21173.9320	21081.1306	20993.9815
91	21260.1665	21172.2644	21083.6233	21264.3033	21170.5451	21082.5552
92	21351.3916	21262.6665	21173.1095	21355.6104	21260.8961	21172.0669
93	21443.5504	21354.0040	21263.5317	21447.8518	21352.1819	21262.5149
94	21536.6412	21446.2753	21354.8883	21541.0259	21444.4010	21353.8979
95	21630.6625	21539.4790	21447.1778	21635.1312	21537.5519	21446.2143
96	21725.6126	21633.6134	21540.3986	21730.1660	21631.6329	21539.4626
97	21821.4901	21728.6769	21634.5493	21826.1287	21726.6426	21633.6412
98	21918.2933	21824.6679	21729.6282	21923.0177	21822.5794	21728.7486
99	22016.0204	21921.5849	21825.6338	22020.8315	21919.4415	21824.7831
100	22114.6700	22019.4261	21922.5645	22119.5682	22017.2274	21921.7432

TABLE III. See Appendix B.

J	F3	F2	F1
1			−99.0694
2		−0.1708	−96.9575
3	104.6354	3.0336	−93.7897
4	108.9502	7.3061	−89.5661
5	114.3435	12.6467	−84.2866
6	120.8154	19.0552	−77.9513
7	128.3656	26.5316	−70.5603
8	136.9940	35.0756	−62.1136
9	146.7005	44.6874	−52.6114
10	157.4849	55.3666	−42.0536
11	169.3470	67.1131	−30.4404
12	182.2867	79.9268	−17.7719
13	196.3036	93.8075	−4.0483
14	211.3976	108.7550	10.7305
15	227.5685	124.7691	26.5641
16	244.8158	141.8495	43.4525
17	263.1394	159.9960	61.3956
18	282.5389	179.2083	80.3931
19	303.0140	199.4863	100.4448
20	324.5643	220.8295	121.5506
21	347.1895	243.2377	143.7103
22	370.8892	266.7106	166.9237
23	395.6630	291.2478	191.1905
24	421.5105	316.8490	216.5105
25	448.4312	343.5139	242.8835
26	476.4247	371.2420	270.3092
27	505.4905	400.0330	298.7873
28	535.6282	429.8864	328.3175
29	566.8373	460.8019	358.8996
30	599.1171	492.7790	390.5332
31	632.4673	525.8172	423.2181
32	666.8871	559.9162	456.9538
33	702.3762	595.0754	491.7401
34	738.9338	631.2943	527.5766
35	776.5595	668.5724	564.4629
36	815.2525	706.9093	602.3986
37	855.0122	746.3043	641.3833
38	895.8381	786.7570	681.4167
39	937.7294	828.2667	722.4983
40	980.6854	870.8329	764.6276
41	1024.7055	914.4549	807.8043
42	1069.7890	959.1323	852.0277
43	1115.9352	1004.8644	897.2976
44	1163.1432	1051.6504	943.6133
45	1211.4124	1099.4899	990.9743
46	1260.7419	1148.3821	1039.3802
47	1311.1311	1198.3263	1088.8304
48	1362.5790	1249.3219	1139.3244
49	1415.0850	1301.3682	1190.8615
50	1468.6481	1354.4643	1243.4412
51	1523.2676	1408.6097	1297.0629
52	1578.9425	1463.8035	1351.7259
53	1635.6720	1520.0451	1407.4298
54	1693.4552	1577.3335	1464.1737
55	1752.2913	1635.6681	1521.9572
56	1812.1792	1695.0479	1580.7794
57	1873.1182	1755.4723	1640.6397
58	1935.1071	1816.9404	1701.5374
59	1998.1452	1879.4513	1763.4718
60	2062.2314	1943.0042	1826.4422
61	2127.3647	2007.5981	1890.4478
62	2193.5442	2073.2323	1955.4878
63	2260.7688	2139.9057	2021.5614
64	2329.0376	2207.6176	2088.6680
65	2398.3494	2276.3669	2156.8066
66	2468.7032	2346.1527	2225.9764
67	2540.0980	2416.9740	2296.1766
68	2612.5327	2488.8300	2367.4064
69	2686.0062	2561.7195	2439.6648
70	2760.5173	2635.6416	2512.9509
71	2836.0651	2710.5953	2587.2640
72	2912.6483	2786.5795	2662.6030
73	2990.2658	2863.5932	2738.9670
74	3068.9164	2941.6353	2816.3551
75	3148.5990	3020.7048	2894.7663
76	3229.3123	3100.8006	2974.1995
77	3311.0553	3181.9216	3054.6539
78	3393.8266	3264.0666	3136.1285
79	3477.6251	3347.2345	3218.6220
80	3562.4495	3431.4242	3302.1336
81	3648.2985	3516.6346	3386.6622
82	3735.1710	3602.8643	3472.2067
83	3823.0655	3690.1124	3558.7660
84	3911.9808	3778.3775	3646.3389
85	4001.9157	3867.6585	3734.9244
86	4092.8688	3957.9541	3824.5214
87	4184.8387	4049.2630	3915.1286
88	4277.8241	4141.5841	4006.7449
89	4371.8237	4234.9160	4099.3692
90	4466.8361	4329.2574	4193.0001
91	4562.8599	4424.6071	4287.6366
92	4659.8937	4520.9637	4383.2773
93	4757.9360	4618.3260	4479.9210
94	4856.9855	4716.6924	4577.5665
95	4957.0408	4816.0618	4676.2125
96	5058.1003	4916.4327	4775.8576
97	5160.1626	5017.8037	4876.5006
98	5263.2262	5120.1735	4978.1401
99	5367.2896	5223.5406	5080.7748
100	5472.3514	5327.9036	5184.4034

$$\langle \delta^2\ ^1\Sigma^+ | H_{so} | B\ ^3\Pi_{0e} \rangle = 2\hat{a}_\delta,$$

where it is supposed that the δ electron is a pure Ti $3d$ (with $l=2$).

If spin–spin interactions are neglected (see their magnitude on Table I), the observed level structure is obtained by diagonalizing the following 3×3 matrix

$$\begin{array}{ccc} |^1\Sigma^+\rangle^0 & |^3\Sigma^-{}_0\rangle^0 & |^3\Pi_{0e}\rangle^0 \end{array}$$
$$\begin{pmatrix} E^0(^1\Sigma^+) & 2\hat{a}_\delta & -\hat{a}_\delta \\ & E^0(^3\Sigma^-{}_0) & \hat{a}_\delta \\ \text{Symmetrical} & & T-A+2/3\lambda+(o+p+q) \end{pmatrix},$$

where the superscript 0 indicates a nonperturbed quantity. The diagonalization gives the calculated values

$$\begin{array}{ccc} |^1\Sigma^+\rangle & |^3\Sigma^-{}_0\rangle & |^3\Pi_{0e}\rangle \end{array}$$
$$\begin{pmatrix} E(^1\Sigma^+) & 0 & 0 \\ & E(^3\Sigma^-{}_0) & 0 \\ \text{Symmetrical} & & T-A+2/3\lambda-(o+p+q) \end{pmatrix}.$$

Unfortunately, the positions of the $^1\Sigma^+$ and $^3\Sigma^-$ states of TiO have not been determined but only roughly evaluated in Ref. 13 as $E(^1\Sigma^+)=14\,000$ cm^{-1} and $E(^3\Sigma^-{}_0)=5000$ cm^{-1}. The diagonalization is possible only if the matrix element $\langle \delta^2,\ ^1\Sigma^+ | H_{so} | \delta^2, ^3\Sigma^- \rangle$ is different from the two matrix elements involving $\langle \delta\ ^{1,3}\Sigma | H_{so} | \delta^2\ \ B\ ^3\Pi \rangle$. Keeping $\langle \delta^2,\ ^1\Sigma^+ | H_{so} | \delta^2,\ ^3\Sigma^- \rangle = 2\hat{a}_\delta = 202.6$ cm^{-1} and taking the integrals involving the $B\ ^3\Pi_{0e}$ level in terms of a new variable parameter $\hat{a}'_\delta$, one obtains an iterative solution correctly reproducing the $^3\Pi_0$ positions if

$$\hat{a}'_\delta = 53.8\ \ \text{cm}^{-1}.$$

This value is about half the expected one, i.e., 101.3 cm^{-1}. This effect, much weaker than in VN,[15] is ascribed to the fact that the 4π m.o. is a mixture of Ti ($3d\pi$) and O ($2p\pi$). Balfour *et al.*[15] have shown, by analogy with the NbN molecule, that the configuration mixing would put some $\sigma^2\ ^1\Sigma^+$ character into the $\delta^2\ ^1\Sigma^+$ state, leading to a reduction of $\hat{a}_\delta$, but this parameter remains much greater than $\hat{a}'_\delta$.

Obviously the Λ doubling interpretation in the TiO $B\ ^3\Pi$ state needs more reliable *ab initio* calculations and also experimental observation of the $^1\Sigma^+$, $^3\Sigma^-$ electronic states and of the $^1\Pi$ state arising from the ($1\delta^2$) and from the $(1\delta)^1$ $(1\pi)^1$ configurations respectively.

VII. CONCLUSION

Owing to the high resolution and to the high signal to noise obtained in the experiment, it has been possible to achieve a detailed analysis of the rotational structure of the $B\ ^3\Pi - X\ ^3\Delta$ (1,0) band of TiO. A set of 24 molecular parameters has been derived. The first-order spin–orbit constants have been interpreted in terms of the electron configurations giving rise to these electronic states.

The $X\ ^3\Delta$ state is well represented by the ...$(8\sigma)^2$ $(3\pi)^4$ $(9\sigma)^1$ $(1\delta)^1$ electron configuration in which the $9\sigma^1$ m.o. is mainly Ti $4s$ and the $1\delta^1$ is a pure Ti $3d$ orbital.

The $B\ ^3\Pi$ state is partly ...$(8\sigma)^2$ $(3\pi)^4$ $(1\delta)^1$ $(4\pi)^1$, where the antibonding 4π orbital is mainly Ti $3d$. The isoconfigurational spin–orbit interaction, partly reproduces the position of the $a\ ^1\Delta$ state but fails totally for the $^1\Pi$ companions of $B\ ^3\Pi$. Moreover the Λ doubling in the $B\ ^3\Pi$ component is not at all explained by the spin–orbit interactions with the states arising from the δ^2 configuration. Clearly, new *ab initio* calculations are necessary to reproduce the observed the TiO spectrum.

ACKNOWLEDGMENT

C.A. is grateful to Professor Anthony J. Merer (University of British Columbia, Canada) for a fruitful correspondence about matrix elements in triplet states and TiO problems.

APPENDIX A: RELATIVE TERM VALUES (IN cm^{-1}) FOR THE TiO $B\ ^3\Pi$ ($v=1$) LEVEL (TABLE II)

F1 is written for $\Omega=0$, F2 for $\Omega=1$, and F3 for $\Omega=2$ spin–orbit sublevels.

APPENDIX B: RELATIVE TERM VALUES (IN cm^{-1}) FOR THE TiO $X\ ^3\Delta$ ($v=0$) LEVEL (TABLE III)

F1 is written for $\Omega=1$, F2 for $\Omega=2$, and F3 for $\Omega=3$ spin–orbit sublevels. See the text for the origin of energies.

[1] P. W. Merrill, A. J. Deutsch, and P. C. Keenan, Astrophys. J. **136**, 21 (1962).
[2] N. M. White and R. F. Wing, Astrophys. J. **222**, 209 (1978).
[3] W. W. Morgan and P. C. Keenan, Annu. Rev. Astron. Astrophys. **11**, 29 (1973).
[4] J. G. Phillips and S. P. Davis, Publ. Astron. Soc. Pac. **99**, 839 (1987).
[5] K. P. Huber and G. Herzberg, *Molecular Spectra and Molecular Structure* (Van Nostrand Reihold, New York, 1979), Vol. 4.
[6] A. J. Merer, Annu. Rev. Phys. Chem. **40**, 407 (1989).
[7] F. P. Coheur, Bull. Soc. R. Sci. Liege, **12**, 98 (1943).
[8] W. H. Hocking, M. C. L. Gerry, and A. J. Merer, Can. J. Phys. **57**, 54 (1979).
[9] T. Gustavsson, C. Amiot, and J. Vergès, J. Mol. Spectrosc. **145**, 56 (1991).
[10] E. M. Azaroual, Thèse Université d'Orsay 1994.
[11] E. M. Azaroual, P. Luc, and R. Vetter, J. Phys. C, **2**, 899 (1992).
[12] S. Gersternkorn and P. Luc, *Atlas du Spectre d'Absorption de la Molécule d'Iode* (Presses du C.N.R.S., ISBN 2-222-03881-2, Laboratoire Aimé Cotton, 1987).
[13] R. N. Zare, A. L. Schmeltekopf, W. J. Harrop, and D. L. Albritton, J. Mol. Spectrosc. **46**, 37 (1973).
[14] J. M. Brown, M. Kaise, C. M. L. Keer, and D. J. Milton, Mol. Phys. **36**, 553 (1978); J. M. Brown, A. E. Colbourn, J. K. G. Watson, and F. D. Wayne, J. Mol. Spectrosc. **74**, 294 (1979).
[15] W. J. Balfour *et al.*, J. Chem. Phys. **99**, 3288 (1988).
[16] C. W. Bauschlicher, Jr., P. S. Bagus, and C. J. Nelin, Chem. Phys. Lett. **191**, 229 (1983).
[17] J. M. Sennesal and J. Schamps, Chem. Phys. **114**, 37 (1987).
[18] A. J. Merer (private communication to C.A.).
[19] H. Lefebvre-Brion and R. W. Field, *Perturbations in the Spectra of Diatomic Molecules* (Academic, Orlando, 1986).